

Quantum Theory of Quantum-Hall Smectics

A.H. MacDonald^{1,2} and Matthew P.A. Fisher²

¹*Department of Physics, Indiana University, Bloomington, IN 47405-4202*

²*Institute for Theoretical Physics, University of California at Santa Barbara, Santa Barbara CA 93106-4030*
(May 9, 2018)

We propose a quantum stripe (smectic) coupled-Luttinger-liquid model for the anisotropic states which occur in two-dimensional electron systems with high-index partial Landau level filling, $\nu^* = \nu - [\nu]$. Perturbative renormalization group calculations establish that interaction terms neglected in this model are relevant - probably driving the system into an anisotropic Wigner crystal—but for $0.4 \lesssim \nu^* \lesssim 0.6$ only below temperatures which are outside of the experimentally accessible range. We argue that the Hall conductance of the ground state flows toward $[\nu]e^2/h$ and $([\nu] + 1)e^2/h$ respectively, on the low and high filling factor sides of this range, consistent with recent observations. A semiclassical theory of smectic state transport properties, which incorporates Luttinger liquid effects in the evaluation of scattering amplitudes, accounts for the magnitude of the dissipative resistivities at $\nu^* = 1/2$, for their ν^* -dependence, and for the observation of non-linearities of opposite sign in easy and hard direction resistivities.

73.40.Hm,73.20.Dx,72.10-d

I. INTRODUCTION

Recent transport experiments^{1–3} have established a qualitative difference between low-energy states of two-dimensional electron systems with large and small index partially filled Landau levels. For Landau level filling factors $\nu < 4$ (orbital Landau level indices smaller than $N = 2$), isotropic quantum Hall fluid states occur at fractional values of ν . For $N \geq 2$, on the other hand, experiments have discovered regions of strongly anisotropic dissipative transport near half-odd-integer filling factors, bracketed by reentrant integer-quantum-Hall effect regions with Hall conductivities $[\nu](e^2/h)$ and $([\nu] + 1)(e^2/h)$. This dependence on N is presumably due to subtle changes in the effective interactions among the electrons of the partially filled Landau level. In this article we describe a theory which accounts qualitatively and often semi-quantitatively for the principle facts uncovered by this series of experiments.

Following Eisenstein and co-workers,¹ we start from the assumption that the true ground state is close to the unidirectional charge-density-wave states proposed for $N \geq 2$ on the basis of Hartree-Fock calculations by Koulakov *et al.*⁴ and Moessner and Chalker.⁵ In Section II we derive a model of coupled one-dimensional chiral Luttinger liquid electron systems for this state. The derivation provides microscopic expressions for the interaction parameters of the model, which are long-range because of the long-range of the underlying Coulomb interaction between electrons. This model neglects small interstripe backscattering terms. In Section III we demonstrate that these terms are technically relevant, but near half filling ($0.4 \lesssim \nu^* \lesssim 0.6$) only at inaccessibly low temperatures. Outside this range, however, observable Wigner crystal instabilities are predicted. In Section III we present an estimate of the ν^* dependence of the tem-

perature below which Wigner crystal states are expected to form. Transport physics in the interesting stripe state regime near $\nu^* = 1/2$ is considered in Section IV. We present a semiclassical theory in which Luttinger liquid effects are incorporated in the evaluation of scattering amplitudes and which describes experiments^{1–3} semi-quantitatively. This theory makes a number of parameter free quantitative predictions which are in good accord with observations. In particular, the product of easy and hard direction resistivities in this theory is independent of disorder strength and has a value which agrees well with experiments. Moreover, Luttinger liquid effects lead to a natural explanation of the non-linear transport effects observed experimentally.

Several recent papers^{6–9} have explored the properties of interacting electron systems in higher Landau levels. The basic framework of our theory has much in common with the work of Fradkin and Kivelson,¹⁰ whose approach intriguingly suggests¹¹ a similarity between the strong correlation physics of quantum Hall and doped Mott insulator systems. These authors have emphasized the intimate relationship (based on shared symmetry properties) between uni-directional charge density wave states and smectic liquid crystal states. We have followed their lead in referring to the anisotropic high Landau level states as quantum-Hall smectics. Both theories identify the electron stripes as one dimensional electron systems and use bosonization techniques to describe the low energy excitations of their left-going and right-going states. The most important difference in our work is that stripe position and shape fluctuations are identified microscopically with the same low energy excitations. They are *not* separate low-energy degrees of freedom. Our theory can be developed in terms of either standard Luttinger liquid boson fields or equivalently in terms of stripe width and position fields. We find one set of gapless collective modes

for quantum-Hall smectics, which encompasses all of the low energy degrees of freedom. A physical consequence of this difference is that in our theory, the quantum-Hall smectic ground state is *always unstable* to the formation of either an electron or a hole Wigner crystal, depending on the sign of $1/2 - \nu^*$.

II. QUANTUM SMECTIC MODEL

The smectic state of Hartree-Fock theory^{4,5} is a single-Slater-determinant with alternating occupied and empty guiding-center occupation-numbers stripes as illustrated schematically in Fig. (1). These states spontaneously break translational and rotational symmetry. For large N they tend to have lower energy than isotropic fluid states because the electrostatic energy penalty, which usually thwarts the phase-separation¹¹ favored by exchange interactions and by electronic correlations, is small^{4,5} when the density wave period is comparable to the cyclotron orbit diameters of index N electrons. We can consider these states to be composed of either electron or hole stripes with right and left going quasiparticles at opposite edges.

Small fluctuations in the positions and shapes of the stripes can be described in terms of particle-hole excitations near the stripe edges. The residual interactions, ignored in Hartree-Fock theory, which scatter into these low energy states fall into two classes: “forward” scattering interactions which conserve the number of electrons on each edge of every stripe, and “backward” scattering processes which do not. The latter processes involve large momentum transfer and will be smaller in magnitude (see below). The quantum smectic model described in this section includes forward scattering only. These interactions are bilinear in the 1d electron densities associated with the chiral currents at the stripe edges: $\rho_{n\alpha}(x)$, with $\alpha = \pm$. As explained in Fig. (1), these densities are proportional to an “elastic” field $u_{n\alpha}(x) = \alpha 2\pi\ell^2 \rho_{n\alpha}(x)$ (with $\ell = (\hbar c/eB)^{1/2}$ the magnetic length), which measures the transverse displacement of a stripe edge relative to its presumed equilibrium position, $y_{n\pm}^0 = a(n \pm \nu^*/2)$. The quadratic Hamiltonian which describes the *classical* energetics for small fluctuations has the following general form:

$$\begin{aligned} H_0 &= \frac{1}{2\ell^2} \int_{x,x'} \sum_{n,n'} u_{n\alpha}(x) D_{\alpha\beta}(x-x'; n-n') u_{n'\beta}(x') \\ &= \frac{1}{2\ell^2} \int_{\mathbf{q}} u_{\alpha}(-\mathbf{q}) D_{\alpha\beta}(\mathbf{q}) u_{\beta}(\mathbf{q}), \end{aligned} \quad (1)$$

where $\int_{\mathbf{q}} \equiv \int d^2\mathbf{q}/(2\pi)^2$. Here the q_y integral is over the interval $(-\pi/a, \pi/a)$ and a high momentum cutoff $\Lambda \sim 1/\ell$ is implicit on q_x .

Symmetry considerations further constrain the form of the elastic kernel. In position space the kernel must be real and symmetric so that, $D_{\alpha\beta}(\mathbf{q}) =$

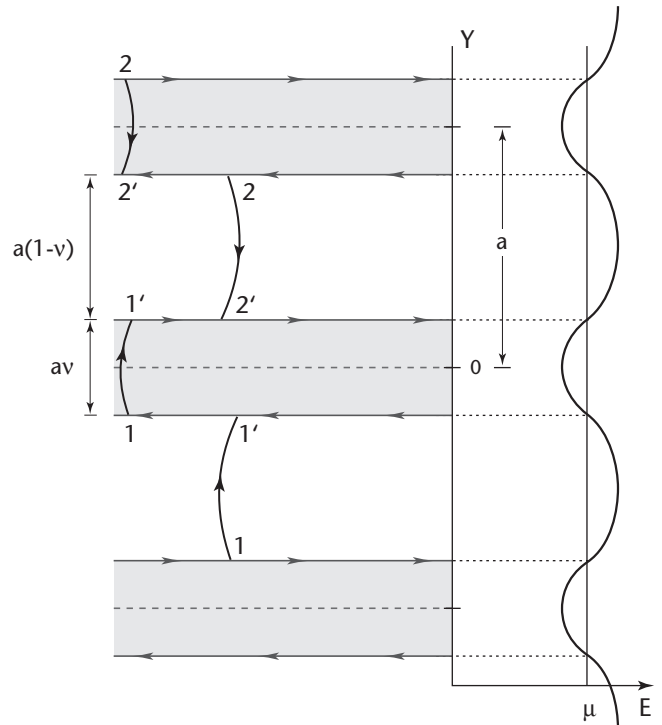


FIG. 1. Schematic illustration of the Hartree-Fock theory smectic state. This state is a local minimum of the Hartree-Fock energy functional for any value of ν^* and any Landau level index. At filling factor ν^* , the occupied Landau gauge single-particle states have guiding centers in stripes of width av^* , shaded in this figure, which repeat with period a . The state can be viewed as consisting of periodically repeated electron stripes or hole stripes. The Hartree-Fock single-particle eigenvalues lie below the Fermi level for guiding centers in the stripes and above the Fermi level for guiding centers outside the stripes. We take the \hat{x} direction to be along the stripes and the \hat{y} direction to be across the stripes. In a magnetic field, the guiding center is related to wavevector by $k = y/\ell^2$ where ℓ is the magnetic length. Each stripe has right and left-going Hartree-Fock quasiparticles at its top and bottom edges respectively. In the Luttinger liquid theory for the one-dimensional stripes, the local Fermi momentum for left and right going states in each stripe is elevated to a quantum field. Because of the connection between guiding center and momentum, these fields also describe the thermal and quantum fluctuations of the shapes and positions of the electron and hole stripes. The number of right and left going states in any channel is related to its Fermi wavevector by $\rho_{n,\pm} = k_{F,\pm}/2\pi$. The strongest momentum-conserving interaction terms not included in the non-interacting boson limit of the Luttinger liquid theory are those in which electrons scatter from left to right-going states in one electron stripe or hole stripe and from right to left-going states in a different stripe of the same type.

$D_{\alpha\beta}^*(-\mathbf{q}) = D_{\beta\alpha}^*(\mathbf{q})$. This implies $D_{-+}(\mathbf{q}) = D_{+-}^*(\mathbf{q})$ and $\text{Im}D_{\alpha\alpha}(\mathbf{q}) = 0$. Parity invariance (under $x, n, + \leftrightarrow -x, -n, -$), implies moreover $D_{++}(\mathbf{q}) = D_{--}(\mathbf{q})$. Thus, the elastic kernel is fully specified by one real function, $D_{++}(\mathbf{q})$, and one complex function, $D_{+-}(\mathbf{q})$. In the *g-ology* notation of the 1D electron gas literature^{12,13} these amplitudes correspond to g_4 and g_2 , respectively. Finally, provided the broken translational and rotational invariance in the smectic occur spontaneously, the classical Hamiltonian must be invariant under: $u_{n\alpha}(x) \rightarrow u_{n\alpha}(x) + \text{const}$ and $\partial_x u_{n\alpha}(x) \rightarrow \partial_x u_{n\alpha}(x) + \text{const}$. This symmetry determines the form of $D(\mathbf{q}) = \sum_{\alpha\beta} D_{\alpha\beta}(\mathbf{q})$ at small wavevector:

$$D(\mathbf{q}) = K_x q_x^4 + K_y q_y^2 + \dots, \quad (2)$$

the characteristic form for smectic elasticity.

A *quantum* theory of the quantum-Hall smectic is obtained by imposing Kac-Moody commutation relations on the chiral densities:

$$[\rho_{n\alpha}(x), \rho_{n'\beta}(x')] = \frac{i}{2\pi} \alpha \delta_{\alpha,\beta} \delta_{n,n'} \partial_x \delta(x - x'). \quad (3)$$

This commutator together with H_0 fully specifies the quantum dynamics. Electron operators in the chiral edge modes are related to the 1d densities via the usual bosonic phase fields: $\psi_{n\alpha} \sim e^{i\phi_{n\alpha}}$ with $\rho_{n\alpha} = \alpha \partial_x \phi_{n\alpha} / 2\pi$. It is a notable feature of the strong field regime that the Luttinger liquid bosonic fields, $\phi_{n,\pm}(x)$, fully determine the stripe position and shape fluctuations. In terms of the bosonic fields, the local center of the n^{th} stripe is

$$\begin{aligned} Y_n(x) &= an + \frac{u_{n,+}(x) + u_{n,-}(x)}{2} \\ &= an + \frac{\ell^2 [\partial_x \phi_{n,+}(x) + \partial_x \phi_{n,-}(x)]}{2} \end{aligned} \quad (4)$$

and the local width of the n^{th} stripe is

$$\begin{aligned} W_n(x) &= av^* + u_{n,+}(x) - u_{n,-}(x) \\ &= av^* + \ell^2 [\partial_x \phi_{n,+}(x) - \partial_x \phi_{n,-}(x)] \end{aligned} \quad (5)$$

We also remark that even though H_0 has a quadratic form, there is no limit in which a free Fermion description of the smectic (with $D_{\alpha\beta}(n) \sim \delta_{\alpha\beta} \delta_{n0}$) is valid. The interactions which are responsible for the broken symmetry play an essential role.

Quantum properties of the smectic can be computed from the imaginary-time action,

$$\begin{aligned} S_0 &= \int_{x,\tau} \frac{1}{4\pi} \sum_{n,\alpha} i\alpha \partial_\tau \phi_{n,\alpha} \partial_x \phi_{n,\alpha} + \int_\tau H_0 \\ &= \frac{1}{2} \int_{\mathbf{q},\omega} \phi_\alpha(-\mathbf{q}, -\omega) M_{\alpha,\beta}(\mathbf{q}, \omega) \phi_\beta(\mathbf{q}, \omega), \end{aligned} \quad (6)$$

where in an obvious matrix notation,

$$\mathbf{M}(\mathbf{q}, \omega) = (i\omega q_x / 2\pi) \boldsymbol{\sigma}^z + (q_x \ell)^2 \mathbf{D}(\mathbf{q}). \quad (7)$$

Correlation functions follow from Wick's theorem and the momentum space correlator $\langle \phi_\alpha \phi_\beta \rangle = \mathbf{M}^{-1}$ with

$$\mathbf{M}^{-1}(\mathbf{q}, \omega) = \boldsymbol{\sigma}_z \mathbf{M}(\mathbf{q}, -\omega) \boldsymbol{\sigma}_z / \det \mathbf{M}(\mathbf{q}, \omega). \quad (8)$$

Due to the spontaneous breaking of translational and rotational symmetry in the smectic, one expects gapless Goldstone modes at zero wavevector. The collective mode dispersion is readily obtained by setting $\det \mathbf{M}(\mathbf{q}, i\omega_{\mathbf{q}}) = 0$ giving $\omega_{\mathbf{q}} = v(\mathbf{q}) q_x$ with a velocity,

$$v(\mathbf{q}) = (2\pi \ell^2) [D_{++}^2(\mathbf{q}) - |D_{+-}(\mathbf{q})|^2]^{1/2}. \quad (9)$$

At small wavevectors, the mode velocity vanishes: $v^2(\mathbf{q}) \sim q_y^2 + q_x^4$. Internal consistency requires that these soft modes do *not* restore the symmetries assumed to have been broken in the smectic state. To examine this we consider the complex smectic order parameter, $\Phi \sim e^{iQ u}$, which describes the charge-density order: $\delta\rho = \text{Re} \Phi e^{iQ y}$ with $Q = 2\pi/a$ the ordering wavevector. The average $\langle \Phi \rangle$ can be readily computed using the quantum harmonic theory, and at $T = 0$ one finds $\langle \Phi \rangle \sim \exp(-Q^2 I)$ with

$$I \sim \int_{\mathbf{q}} |q_x| D_{++}(\mathbf{q}) / v(\mathbf{q}). \quad (10)$$

With D_{++} non-zero at $\mathbf{q} = 0$, the integrals converge at small \mathbf{q} , so that the deBye-Waller factor ($e^{-Q^2 I}$) and smectic order parameter are non-vanishing. Evidently, these harmonic quantum fluctuations are insufficient to destroy the broken symmetries in the smectic.¹⁴

The effect of the neglected backscattering interactions, considered in the next Section, depends sensitively on the elastic constants at $q_x = 0$. In this limit the relevant excited states are simply Slater determinants with straight stripe edges displaced from those of the Hartree-Fock theory ground state. By evaluating the expectation value of the microscopic Hamiltonian in a state with arbitrary stripe edge locations we find that

$$D_{\alpha\beta}(q_x = 0, q_y) = \delta_{\alpha\beta} D_0 + \alpha\beta \frac{a}{4\pi^2 \ell^2} \sum_n e^{iq_y a n} \Gamma(y_{n\alpha}^0 - y_{0\beta}^0), \quad (11)$$

where the value of the constant D_0 is such that $\sum_{\alpha\beta} D_{\alpha\beta}(\mathbf{q} = 0) = 0$. Here, $\Gamma(y)$ is the interaction potential between two electrons located in guiding center states a distance y apart:

$$\Gamma(y) = U(0, y/\ell^2) - U(y/\ell^2, 0), \quad (12)$$

$$U(q, k) = \int \frac{dp}{2\pi} e^{-(q^2 + p^2)\ell^2/2} V_{\text{eff}}^N(q, p) e^{-ipk\ell^2}. \quad (13)$$

The two terms in Eq. (12) are direct and exchange contributions. In Eq. (13), $V_{\text{eff}}^N(q, p)$ is the Fourier transform of

III. BACK SCATTERING INTERACTIONS

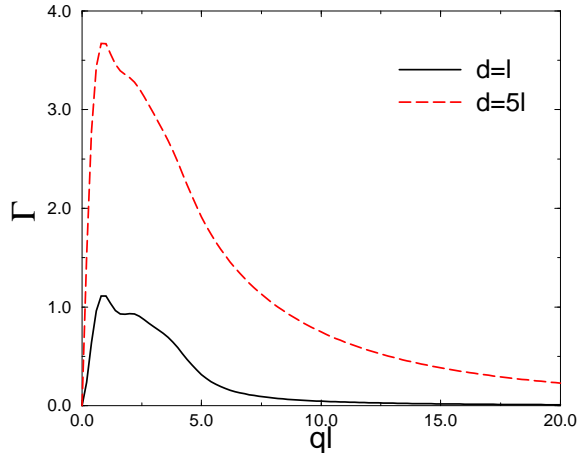


FIG. 2. Interaction matrix element $\Gamma(y)$ vs. dimensionless separation $y/\ell = ql$ for the case of interactions in a zero-width 2D layer screened by a parallel metallic layer and with Landau level index $N = 2$. d is the distance to the metallic layer and Γ is in units of $e^2/\epsilon \approx 200$ meV nm for 2D electron systems formed near the surface of a GaAs crystal. The Luttinger model g-ology parameter which characterizes interactions between stripes separated by na in the 2D electron layer is $\sim \Gamma(na)$. $\Gamma(y)$ is simply related to the elastic constants in terms of which the chiral Luttinger model is developed in the text. Metallic screening layers are sometimes present in experimental samples but are introduced here mainly as a convenience since Γ varies logarithmically with y at large y if they are not present and various sums over stripe indices do not converge. The limit $d \rightarrow \infty$ can be taken at the end of the calculation, if appropriate. Γ vanishes for $y \rightarrow 0$ because its direct and exchange contributions cancel.

the effective 2D electron interaction which incorporates form-factors⁹ dependent on the Landau level index N and the ground subband wavefunction of the host semiconductor heterojunction or quantum well. The smectic states have relatively long periods proportional to the index N cyclotron orbit radii. Explicit calculations^{4,9} show that $a \gtrsim 6\ell$ for $N \geq 2$. It follows that the exchange contribution to $\Gamma(y)$ is small and that $\Gamma(y)$ decreases with stripe separation in the relevant range. With unscreened Coulomb interactions, $\Gamma(y)$ diverges logarithmically at large y , so it is convenient to introduce a metallic screening plane. This changes the large y behavior to y^{-2} , making the sum over n in Eq. 11 convergent. As shown below, however, we do not find that our conclusions change qualitatively when a screening plane is absent. In Fig. (2) we plot $\Gamma(y)$ for $N = 2$ for the cases of thin 2D electron systems separated from metallic screening planes by $d = \ell$ and $d = 5\ell$. Note that $\Gamma(y)$ is monotonically decreasing with positive curvature in the range of interest.

We now consider the “backward” scattering electron interactions, ignored above. The bare matrix elements for these interactions will fall off exponentially with increasing momentum transfer and with increasing separation between the interacting stripes, so we choose here to focus on the smallest momentum transfer. We discuss explicitly only the case of backscattering¹⁵ across electron stripes and across hole stripes, as illustrated schematically in Fig. 1. For a pair of stripes separated by ma , backscattering across an electron stripe can be expressed in a bosonized form,

$$S_1 = \int_{x,\tau} \sum_{n,m} u_m [\exp(i\theta_{n,m}(x,\tau)) + h.c.], \quad (14)$$

where

$$\theta_{n,m} = (\phi_{n,+} - \phi_{n,-}) - (\phi_{n+m,+} - \phi_{n+m,-}). \quad (15)$$

Hole backscattering takes a similar form. Since the effects of backscattering across electron and hole stripes are equivalent under a particle/hole transformation ($\nu^* \leftrightarrow 1 - \nu^*$) we focus exclusively on the former.

The effects of backscattering can be deduced by implementing a simple renormalization group (RG) scheme. Specifically, we integrate out “fast” boson modes ϕ in a shell, with $\Lambda/b < |q_x| < \Lambda$ and ω, q_y unrestricted, and then rescale $q'_x = bq_x$ and $\omega' = b\omega$ leaving q_y unchanged. With an appropriate rescaling of ϕ , this RG transformation leaves the harmonic smectic action, S_0 , invariant. Stability of the smectic fixed point in the presence of backscattering can be tested by considering the lowest order RG flow equation,

$$\partial u_m / \partial t = (2 - \Delta_m) u_m, \quad (16)$$

with $t = \ln b$. Using Eq. (15) and Eq. (8) we find the following expression for the scaling dimension:

$$\Delta_m = 4 \int_{-\pi}^{\pi} \frac{d(qa)}{2\pi} \sin^2(mqa/2) W(q_x = 0, q). \quad (17)$$

Here, W is a “weight” function,

$$W(\mathbf{q}) = \frac{[D_{++}(\mathbf{q}) + \text{Re}D_{+-}(\mathbf{q})]}{[D_{++}^2(\mathbf{q}) - |D_{+-}(\mathbf{q})|^2]^{1/2}}. \quad (18)$$

If the scaling dimension $\Delta_m < 2$ the smectic phase is *unstable*. Fortunately, Δ_m only depends on the elastic constants at $q_x = 0$, so that we can use the microscopic expressions discussed at the end of the previous section for its evaluation.

If the weight function $W(q_y) \leq 1$ in Eq. 17, then $\Delta_m < 2$ and backscattering is relevant. To understand the dependence of $W(q_y)$ on filling factor it is useful to consider $q_y a = 0, \pi$, so that D_{+-} is real and the expression for W simplifies. For $\mathbf{q} = 0$, smectic elasticity

implies $D_{++} + D_{+-} = 0$, so that $W(q_y = 0) = 0$. When $q_y a = \pi$, one has

$$D_{+-}(q_y a = \pi) = \sum_n \frac{(-1)^n a}{4\pi^2 \ell^2} [\Gamma(an + a(1 - \nu^*)) - \Gamma(an + a\nu^*)]. \quad (19)$$

Note that $D_{+-}(q_y a = \pi)$ vanishes, and the weight function equals 1 for $\nu^* = 1/2$. Provided $\Gamma(y)$ is monotonically decreasing with positive curvature for $y \gtrsim a$, $D_{+-}(q_y \pi)$ will be negative for all $\nu^* < 1/2$, implying $W(q_y a = \pi) < 1$. If the weight function is monotonic in $q_y a$, the backscattering interactions will thus be relevant. Using Eq. (11) and Eq. (12) we have computed $W(q_y)$ for a range of values of N , ν^* , and d , and have always found that it is indeed monotonic; the typical behavior is illustrated in Fig. (3). For the sake of definiteness we have ignored the finite width of the ground subband wavefunction in these calculations. Numerically calculated scaling dimensions for $m = 1$, $N = 2$, and $d = 10\ell$, are plotted in Fig. (4). For $\nu^* > 1/2$, $W(q_y a = \pi) > 1$ so that the electron backscattering amplitude scaling dimension increases, eventually crossing above 2, as seen in Fig. (4). The dependence of the calculated scaling dimension on the distance to the screening plane is illustrated in Fig. (5) for the case $N = 2$ and $\nu^* = 0.5$. As the distance to the screening plane increases the weighting function approaches 1 more rapidly as $q_y a$ goes from 0 to π . However the values at $q_y a = 0, \pi$ are fixed at 0 and 1 respectively, and the curves are monotonic at all values of d . As a result the scaling dimension is only weakly dependent on d and the interaction remains relevant for any finite value of d .

The most significant conclusion which follows from this calculation is that for *all* ν^* , backscattering across either electron or hole stripes is relevant, and will destabilize the smectic ground state. The ultimate fate of the ground state will presumably depend on the relative magnitudes of the various backscattering interactions. For the interactions considered above the bare coupling constants will fall rapidly with increasing stripe separation m :

$$u_m \sim U(av/\ell^2, ma/\ell^2), \quad (20)$$

so that $m = 1$ will dominate. If each electron stripe is viewed as a 1d conductor, this is a $2k_F$ backscattering interaction, which tends to drive¹⁰ charge ordering *along* the stripe, with wavelength corresponding to the 1d electron spacing. We thus strongly suspect that for $\nu^* < 1/2$ the smectic will be unstable to the formation of an electron Wigner crystal, with one electron per unit cell. For large Landau index N , the crystal would be highly anisotropic, compressed along the x -direction, with an aspect ratio proportional to N . For $\nu^* > 1/2$, though, backscattering across the hole stripes will dominate, leading to an anisotropic hole Wigner crystal, with one hole per unit cell. In either crystal phase there will, in contrast to the smectic case, be an energy gap, E_g ,

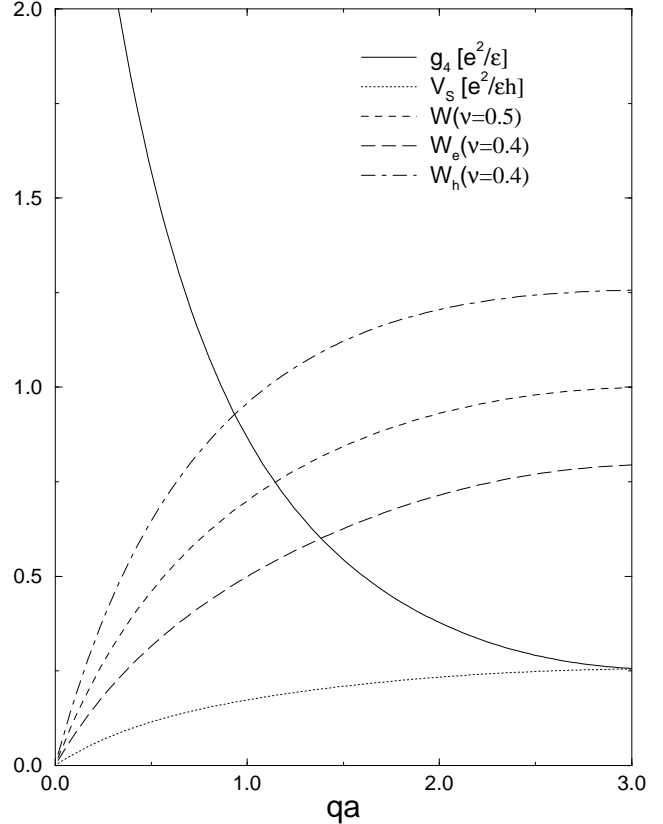


FIG. 3. Quantum-Hall smectic Luttinger model parameters and integrands of the expressions for the backscattering interaction scaling dimensions. This plot is for valence Landau level index $N = 2$ and screening layer distance $d = 10\ell$. $g_4(q)$ is in units of e^2/ϵ and the collective excitation velocity for $\nu^* = 0.5$, $v_S(q_x = 0, q_y q)$ is in units of $e^2/2\pi\epsilon\hbar$. The values of these units are approximately 200meV nm and 4.8×10^4 m/s respectively for 2D electron systems formed near the surface of a GaAs crystal. Our scaling dimension results can be understood in terms of the properties of the weighting factors W in the integrals, as discussed in the text. $g_4(q)$ is related the elastic constants in terms of which the chiral Luttinger model is developed in the text by $D_{++}(k_x = 0, q) = (a/4\pi^2\ell^2)g_4(q)$. The large value of $g_4(q)$ for $q \rightarrow 0$ is due to the long-range of the underlying Coulomb interaction between electrons.

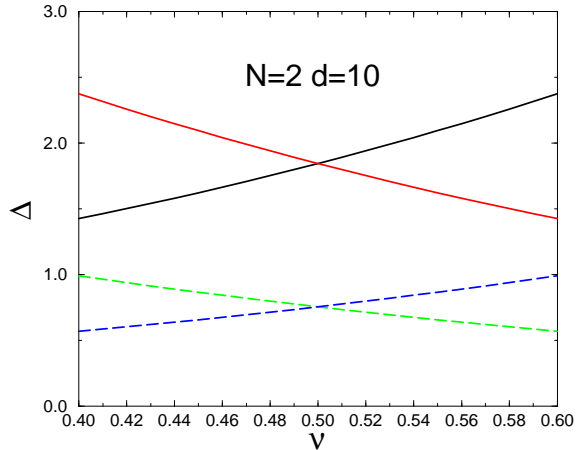


FIG. 4. Scaling dimensions for $m = 1$ electron and hole $2k_F$ scattering and electron and hole impurity scattering vertices (dashed lines) for a range of filling factor near $\nu^* = 1/2$. For this calculation the distance to the screening plane was chosen to be $d = 10\ell$. Electron scattering vertices are an increasing function of filling factor and hole vertices are a decreasing function of filling factor as discussed in the text. The interaction terms are relevant for scaling dimensions smaller than 2 while impurity terms are relevant for scaling dimensions smaller than 1.5. The interedge scattering rate is enhanced at low energies when the impurity interaction scaling dimension is smaller than 1.0. Interaction terms with m larger than one are more relevant but have bare coupling constants which are smaller by several orders of magnitude. Interaction terms with larger momentum transfers than those discussed here also have much smaller bare coupling constants.

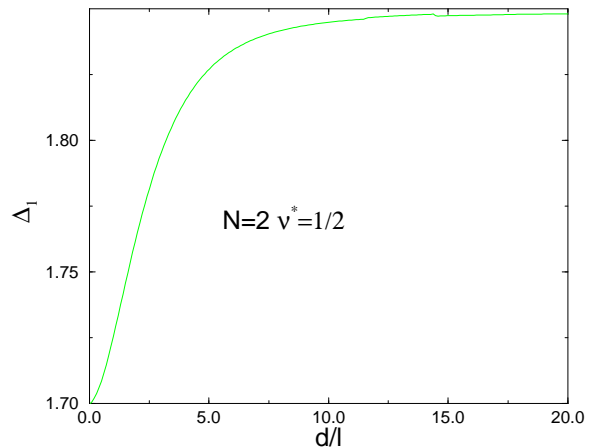


FIG. 5. Dependence of $m = 1$ $\nu^* = 1/2$ electron and hole backscattering amplitude scaling dimensions ($\Delta_{1,e} = \Delta_{1,h} = \Delta_1$) on distance between the two-dimensional electron system and the model's metallic screening plane. Here d is in units of the magnetic length ℓ . For $d \rightarrow 0$, Δ approaches $16/3\pi$, the value which can be calculated analytically for the case of interactions only between nearest neighbor chiral edge modes. As explained in the text, Δ increases with d , but only slowly, and is smaller than 2 for arbitrarily large d .

for single particle excitations. Provided the crystalline order is pinned by the boundaries, these Wigner crystal phases should have vanishing dissipative conductivities σ_{xx} and σ_{yy} . However, the hole Wigner crystal will have an extra Landau level edge state. The quantized Hall conductances of electron and hole Wigner crystal states will be, $\sigma_{xy} = [\nu]e^2/h$ and $[\nu + 1]e^2/h$ respectively.

Of considerable interest is the *magnitude* of the Wigner crystal gap as a function of ν^* . With knowledge of the dimensionless backscattering interaction, u , this gap can be estimated by integrating the RG flow equations. Specifically, under an RG transformation, the energy gap should rescale as,

$$E_g(u) = b^{-1} E_g(b^{2-\Delta} u), \quad (21)$$

with $\Delta = \Delta_1$. When the interaction becomes of order one, $b^{2-\Delta} u = 1$, the energy gap should be roughly equal to the characteristic Coulomb energy, E_c , giving,

$$E_g(u) = (U/E_c)^{1/(2-\Delta)} E_c, \quad (22)$$

with $U = uE_c$ the (dimensionful) backscattering strength. The ν^* dependence of the gap enters both through U , which is extremely small for ν^* near $1/2$ because of the long period of the stripe lattice, and the scaling dimension, Δ , which is maximal at $\nu^* = 1/2$. [For $\nu^* > 1/2$ the same applies to backscattering across hole stripes.] Both effects conspire to *strongly* reduce the gap magnitude near half-filling. Using the above estimates, it is possible to obtain the ν^* dependence of the gap explicitly. Taking $E_c = 0.3e^2/\ell$, the order of the maximum correlation energy per electron in a partially filled Landau level, the resulting gap for $N = 2$ and $d = 10\ell$ is shown in Fig. (6). Notice that the Wigner crystal gap plummets rapidly to extremely small values near $\nu^* = 1/2$, dropping below the range accessible to dilution fridges over the filling factor range $0.4 \lesssim \nu^* \lesssim 0.6$, where anisotropic transport is observed in low-temperature experiments. In this region the Wigner crystal states will be inaccessible (melted at experimental temperatures), and the anisotropic transport of the smectic phase should be unmasked. Outside of this range, the Wigner crystal will be pinned by even weak impurities, resulting in quantized Hall plateaus. For $\nu^* = 0.3$, the gap values estimated here are typical^{1,2} of those found on the reentrant integer quantum Hall plateaus which bracket the anisotropic transport regimes.

We remark that electron and hole Wigner crystal states are also the ground states in the Hartree-Fock approximation.^{9,10,17} In that approximation, however, the gaps are orders of magnitude larger $\sim E_c \simeq 0.3 e^2/\ell$ over a wide-range of filling factors. The Hartree-Fock approximation is expected to be reasonably accurate for the nearly classical Wigner crystal states which occur in the tails of $N \leq 1$ Landau levels. Evidently quantum fluctuations have a larger importance for these $N \geq 2$ crystal states.

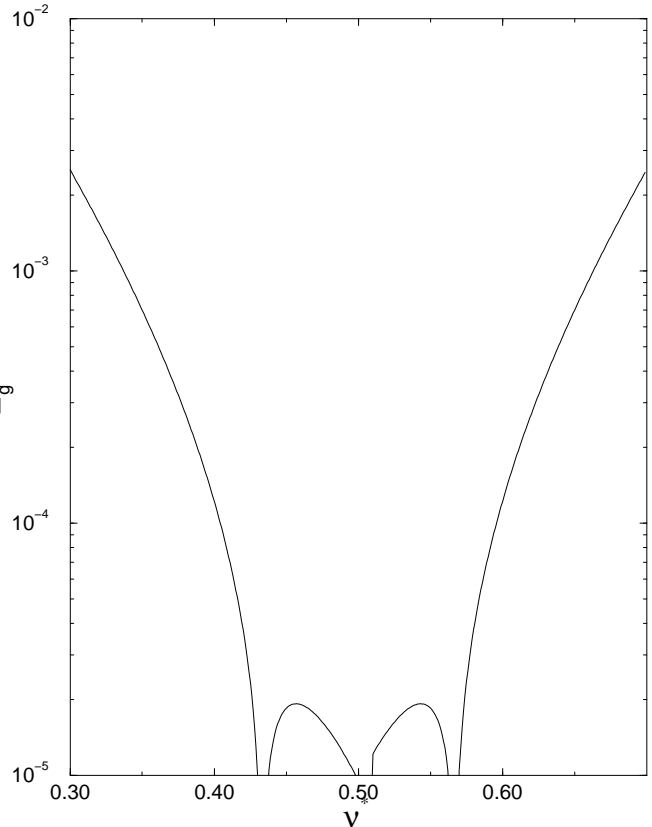


FIG. 6. Estimated single-particle energy gap of the anisotropic Wigner crystal state, E_g , as a function of partial filling factor ν^* for a model with orbital Landau level index $N = 2$ and distance to screening plane $d = 10\ell$. For this model the bare backscattering matrix element vanishes for $\nu^* \sim 0.43$ and $\nu^* \sim 0.57$. These results were obtained with the choice $E_c = 0.3e^2/\ell$. The energy gaps are in units of $e^2/\epsilon\ell$ which has a typical value $\sim 100\text{K}/k_B$. E_g/k_B is smaller than $\sim 10\text{mK}$, the base temperature scale for a dilution fridge, for $0.4 \lesssim \nu^* \lesssim 0.6$. E_g/k_B approaches $\sim 1\text{K}$, the energy gap observed on reentrant integer quantum Hall plateaus, for $\nu^* \sim 0.25$ and $\nu^* \sim 0.75$.

IV. ANISOTROPIC TRANSPORT PROPERTIES

Transport near $\nu^* = 1/2$ in the smectic regime will be strongly influenced by impurities, which are in fact necessary to get *any* transport in the “hard” y -direction. The dominant effect will presumably come from impurity scattering across electron or hole stripes, with the latter being the bottleneck when $\nu^* < 1/2$ and the former when $\nu^* > 1/2$. For weak impurity scattering it is possible to examine their effects perturbatively. Consider for example impurity scattering across electron stripes,

$$H_{imp} = \int_x \sum_n \xi_n(x) e^{i(\phi_{n+} - \phi_{n-})} + h.c., \quad (23)$$

with $\xi(x)$ a complex random potential. Taking $\xi_n(x)$ to be uncorrelated and Gaussian,

$$[\xi_n^*(x) \xi_{n'}(x')]_{ens} = \mathcal{D} \delta_{nn'} \delta(x - x'), \quad (24)$$

a simple RG perturbative in the variance \mathcal{D} is possible. One finds, $\partial \mathcal{D} / \partial t = (3 - 2\Delta_e) \mathcal{D}$, with the scaling dimension of the operator $e^{i(\phi_+ - \phi_-)}$ given by,

$$\Delta_e = \int_{-\pi}^{\pi} \frac{d(qa)}{2\pi} W(q_x = 0, q). \quad (25)$$

Here W is the *same* “weight” function as in Eq. 17. The filling factor dependence of Δ_e can be understood from considerations similar to those for the backscattering amplitudes detailed in the previous section. For 1D non-interacting electrons $\Delta_e = 1$, so that disorder is relevant and eventually leads to localization. For the smectic we can estimate Δ_e as a function of filling ν^* ; the result of this calculation was included in Fig. (4). At all ν^* impurity scattering across either electron or hole stripes is more relevant than in the non-interacting electron case.

In the strict zero temperature limit, we thus expect that impurities (aided by interactions) will ultimately drive localization for all ν^* , except right at the $\nu^* = 1/2$ plateau transition. However, samples in which quantum-Hall smectic physics is observed have extremely weak impurity scattering, so that it might be possible to ignore localization effects at accessible temperatures. More specifically, consider the dimensionless disorder strength, $D = \mathcal{D} \ell / E_c^2$, with E_c the Coulomb energy scale. Provided $D \ll 1$, there should be a large temperature range over which impurity backscattering can be treated perturbatively and localization effects ignored. To see this, it is convenient to introduce an *effective* temperature-dependent disorder strength that follows from the RG; $D_{\text{eff}}(T) = (T/E_c)^{2\Delta_e - 3} D$, which increases upon cooling. Provided $D_{\text{eff}}(T) < 1$, localization effects should be negligible, and Boltzmann transport should be operative.

A key parameter in a Boltzmann approach is the impurity scattering rate Γ_e (Γ_h) across an electron (hole) stripe. Within a simple free-fermion Golden-rule calculation one expects $\Gamma_e^0 = c D E_c$ (with c an order one constant), which is independent of temperature. But under the RG transformation the scattering rate rescales as,

$$\Gamma_e(D, T) = b^{-1} \Gamma_e(b^{3-2\Delta_e} D, bT). \quad (26)$$

Running the RG until $bT = E_c$ gives, $\Gamma(D, T) = (T/E_c) \Gamma(D_{\text{eff}}, E_c)$. Using the free-fermion result at $T = E_c$ one has

$$\Gamma_e(T) = c T D_{\text{eff}}(T) = \Gamma_e^0 (T/E_c)^{2\Delta_e - 2}. \quad (27)$$

This should be valid provided that $D_{\text{eff}} < 1$. For a non-interacting 1D electron gas $\Delta_e = 1$ so that Γ_e is temperature independent. In contrast, Luttinger liquid effects in the quantum Hall smectic give a temperature dependence to the Boltzmann scattering rate - generally increasing upon cooling. Equivalently, the impurity mean free path varies with temperature, in marked contrast to low temperature metallic transport.

In the Boltzmann approach to transport in the quantum Hall smectic that we develop below, quantum interference effects between successive inter-edge impurity backscattering events are ignored. This is valid provided, Γ_e is not large compared to Γ_ϕ , where Γ_ϕ is the electron phase breaking rate. Within a single chiral edge mode, forward scattering interactions will rapidly dephase an electron. A simple perturbative calculation for the electron self energy is expected to give the form; $\Gamma_\phi = c' T u_f^2$ with u_f a dimensionless forward scattering amplitude and c' of order one. Since u_f is also of order one this implies, $\Gamma_\phi = c_\phi T$. Comparing with Eq. 27, one sees that it is thus legitimate to ignore interference between successive impurity backscattering events provided $D_{\text{eff}}(T)$ is not large compared to one. For temperatures low enough that $D_{\text{eff}}(T)$ is large, quantum interference effects cannot be neglected and one expects an onset of localization (except right at $\nu^* = 1/2$). In strong field, the leading one-loop weak localization effects will not be operative, so that two-loop interference processes will drive the localization.

With this preamble in hand, we proceed to develop a semiclassical Boltzmann transport theory for the quantum Hall smectic phase. We assume that the charge density wave itself is pinned and immobilized by both the edges of the sample and weak impurities which couple to the electrons within the stripes. In this case, collective sliding motion of the charge-density will be absent, and the electrical transport will be dominated by single-particle inter-edge electron tunneling. It is convenient to characterize the non-equilibrium current-carrying state by separate local steady state chemical potentials, $\mu_{n\pm}$, for left and right going electrons in each stripe. Due to the discrete translational symmetry of the smectic, the steady state chemical potential must increase by $e E_y a$ upon translation by one period, with E_y the y -component of a (uniform) electric field. Taking the zero of chemical potential as the center of the $n = 0$ electron stripe, we can thus write,

$$\begin{aligned} \mu_{n,+} &= n e E_y a + \mu/2, \\ \mu_{n,-} &= n e E_y a - \mu/2. \end{aligned} \quad (28)$$

Here the chemical potential drops across electron and hole stripes are μ and $eE_y a - \mu$ respectively. An electric field E_x in the \hat{x} direction, induces a steady flow in momentum space which moves each electron stripe to smaller y (for $E_x > 0$), lowering the chemical potential on right-going edges and raising it on left-going edges. This disequilibrium induces a tunneling current across both electron and hole stripes, which attempts to restore equilibrium:

$$\begin{aligned}\dot{\mu}_{n,+} &= -eE_x v_F + \frac{\mu_{n,-} - \mu_{n,+}}{\tau_e} + \frac{\mu_{n+1,-} - \mu_{n,+}}{\tau_h}, \\ \dot{\mu}_{n,-} &= eE_x v_F + \frac{\mu_{n,+} - \mu_{n,-}}{\tau_e} + \frac{\mu_{n-1,+} - \mu_{n,-}}{\tau_h}.\end{aligned}\quad (29)$$

Here, we have introduced inter-edge scattering times, related to the rates above via: $\Gamma_e = 1/\tau_e$ and $\Gamma_h = 1/\tau_h$, for tunneling across electron and hole stripes, respectively. The electric field, E_x , induces a drift in the wavevector of the electrons in each chiral edge mode, $\hbar\dot{k} = -eE_x$. In Eq. (29) v_F is a ‘‘Fermi velocity’’, which relates changes in the edge chemical potential to wavevector: $v_F = \partial\mu/\partial k$. This velocity is determined by the ‘‘onsite’’ piece of the smectic elastic constants as, $v_F = 2\pi\ell^2 D_{++}(q_x = 0, n = 0)$.

In the steady state $\dot{\mu}_{n,\pm} = 0$ so that

$$\mu(\tau_e^{-1} + \tau_h^{-1}) = \frac{eE_y a}{\tau_h} - eE_x v_F, \quad (30)$$

relating the unknown parameter μ to the electric fields. The current in the \hat{x} direction is due to the imbalance between left-going and right-going electrons in each stripe

$$I_x = \frac{e^2}{h} \left[\frac{L_y}{a} \right] (-\mu/e). \quad (31)$$

In Eq. (31) the contribution from each stripe is given by the familiar expression for the quantum Hall current and the factor in square brackets is the number of electron stripes in a sample with width L_y . The current in the \hat{y} direction is equal to the tunneling current across the hole stripes:

$$I_y = \frac{eL_x}{v_F h} \frac{eE_y a - \mu}{\tau_h}. \quad (32)$$

with L_x the sample width. The first factor on the right-hand-side of Eq. (32) is the charge per unit energy in a chiral 1D electron system of length L_x .

Inserting Eq. (30) in Eq. (31) and Eq. (32) to eliminate μ gives the desired expressions for the conductivity matrix,

$$\begin{aligned}\sigma_{xx} &= \frac{e^2}{h} \frac{v_F \tau_e \tau_h}{a(\tau_e + \tau_h)}, \\ \sigma_{yy} &= \frac{e^2}{h} \frac{a}{v_F(\tau_e + \tau_h)}, \\ \sigma_{yx} &= -\sigma_{xy} = \frac{e^2}{h} \left([\nu] + \frac{\tau_e}{\tau_e + \tau_h} \right).\end{aligned}\quad (33)$$

Inverting the conductivity matrix gives the following expressions for the resistivities:

$$\begin{aligned}\rho_{\text{easy}} &= \frac{h}{e^2} \frac{1}{\tau_e([\nu] + 1)^2 + \tau_h[\nu]^2} \frac{a}{v_F} \\ \rho_{\text{hard}} &= \frac{h}{e^2} \frac{1}{\tau_e([\nu] + 1)^2 + \tau_h[\nu]^2} \frac{v_F \tau_e \tau_h}{a} \\ \rho_{\text{hall}} &= \frac{h}{e^2} \frac{1}{\tau_e([\nu] + 1)^2 + \tau_h[\nu]^2} ([\nu] + 1)\tau_e + [\nu]\tau_h,\end{aligned}\quad (34)$$

where $\rho_{\text{easy}} = \rho_{xx}$, $\rho_{\text{hard}} = \rho_{yy}$, and $\rho_{\text{hall}} = \rho_{xy}$.

Eq. (34) relates the dissipative and Hall resistivities to the two scattering rates, Γ_e and Γ_h . The dependencies on temperature and filling factor ν^* enter through these scattering rates, in the form established above:

$$\begin{aligned}\Gamma_e &= \frac{1}{\tau_e} = \Gamma_e^{(0)} (k_B T / E_c)^{2\Delta_e - 2}, \\ \Gamma_h &= \frac{1}{\tau_h} = \Gamma_h^{(0)} (k_B T / E_c)^{2\Delta_h - 2}.\end{aligned}\quad (35)$$

Here, the free-fermion scattering rates across electron and hole stripes, $\Gamma_e^{(0)}$ and $\Gamma_h^{(0)}$, depend on the impurity scattering strength (and ν^*) but *not* the temperature. E_c is the Coulomb energy scale which serves as a high energy cutoff. The scaling dimensions, Δ_e and Δ_h , depend sensitively on ν^* as shown in Fig. (4). As we shall see, these equations describe much of the phenomenology¹⁻³ of transport in quantum Hall stripe states.

Remarkably, for $\nu^* = 1/2$ this theory makes two parameter free quantitative predictions:

$$\rho_{\text{easy}} \rho_{\text{hard}} = (h/e^2)^2 \frac{1}{\left[([\nu] + 1)^2 + [\nu]^2\right]^2}, \quad (36)$$

and

$$\rho_{\text{hall}} = \frac{h}{e^2} \frac{2[\nu] + 1}{([\nu] + 1)^2 + [\nu]^2}. \quad (37)$$

Notice that the scattering times have completely dropped out of these expressions! Interestingly, the Hall resistivity at $\nu = [\nu] + 1/2$ is predicted to deviate noticeably from (the classical value) $(h/e^2)/([\nu] + 1/2)$. The most extensive experimental data is for $[\nu] = 4$. In this case, the value predicted for the product of ρ_{easy} and ρ_{hard} appears to agree with the published data to within better than a factor of two, provided one accounts for the particular current paths¹⁶ appropriate for the sample geometry. Experimental verification of the predicted $[\nu]$ dependence of this product would help establish the efficacy of this transport theory.

At $\nu^* = 1/2$, Eq. (34) predicts a weak temperature dependence of the dissipative resistivities. Specifically, due to Luttinger liquid effects which drive an *enhancement* of the inter-edge scattering rate upon cooling (since

$\Delta_e/h < 1$ at $\nu^* = 1/2$), the resistivity in the hard direction should drop slowly with cooling whereas ρ_{easy} should rise.

It is interesting to consider the predicted dependence of the resistivities on filling factor. For $\nu^* < 1/2$, the electron stripes are narrower than the hole stripes and a free-fermion evaluation of the relaxation times would give $\tau_h > \tau_e$. Since Δ_e decreases and Δ_h increases with increasing $1/2 - \nu^*$, the relaxation rate ratio is expected to increase beyond its free-fermion value at lower temperatures. For $\tau_h \gg \tau_e$ we have that $\rho_{\text{hard}} = (h/e^2)(v_F\tau_e/a)/[\nu]^2$. Since τ_e decreases ever more rapidly upon cooling for larger $1/2 - \nu^*$, the hard resistivity is expected to be large at experimental temperatures only over a narrow interval surrounding $\nu^* = 1/2$. Backscattering interactions ignored in this Boltzmann transport theory will only tend to enhance this effect, acting in concert with impurity scattering.

In the same regime of filling factor, with $\tau_h \gg \tau_e$, the Hall resistivity approaches $(h/e^2)/[\nu]$. Moreover, one has $\rho_{\text{easy}} = (h/e^2)/[\nu]^2(v_F\tau_h/a)$ in this limit. Thus, ρ_{easy} also decreases with $1/2 - \nu^*$, because of both bare matrix element and scaling dimension tendencies. Interestingly, for $\nu^* \lesssim 0.4$ the scaling dimension for scattering across hole stripes, Δ_h , becomes *larger* than one (see Fig. (4)). This implies that Γ_h actually decreases upon cooling in this regime, strongly enhancing the one-dimensional nature of the electron stripes and driving localization. But for $\nu^* \lesssim 0.4$ one really must include the strong effects of electron (backscattering) interactions which drive the Wigner crystal instability - again, this acts in concert with impurity affects. Upon cooling within this Wigner crystal regime, the dissipative resistivities should rapidly vanish leaving a quantized Hall resistance. It follows from particle-hole symmetry that $\tau_e(\nu^*) = \tau_h(1 - \nu^*)$ so similar conclusions can be reached for transport properties at $\nu^* > 1/2$.

In Fig. (7), we plot the ρ_{easy} and ρ_{hard} filling factor dependencies predicted by this model for $[\nu] = 4$ and δ -correlated disorder model. Here we have taken $T = 0.003e^2/\ell$ and $E_c = 0.3e^2/\ell$. The disorder strength was chosen to give $\rho_{\text{hard}}/\rho_{\text{easy}} = 10$ at $\nu^* = 0.5$. Notice that ρ_{easy} has a maximum at $\nu^* = 1/2$, not the minimum seen in many experiments. Within the Boltzmann theory this feature depends on the details of the disorder model used; models with only small angle scattering at zero magnetic field tend to give electron relaxation times which decrease and hole relaxation times which increase more rapidly with $1/2 - \nu^*$, changing the shape of these curves. In addition, current-path corrections¹⁶ might be essential in producing the apparent ρ_{easy} minimum at $\nu^* = 1/2$ in experiments. No plausible disorder model in this theory gives ρ_{hard} results which drop to zero as strongly with increasing $1/2 - \nu^*$ as in experiments; we believe that backscattering interactions and localization, both effects neglected here, are playing an important role in driving the resistivities to small values away from $\nu^* = 1/2$.

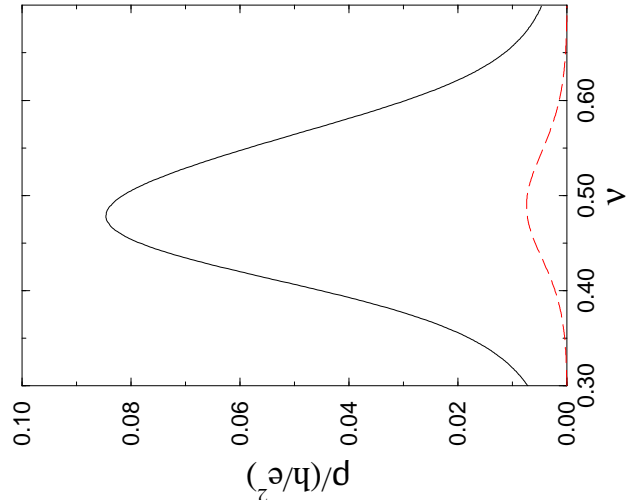


FIG. 7. Linear transport coefficients calculated from the Boltzmann transport theory for $N = 2$ and $d = 10\ell$, using a model of δ -correlated disorder. The disorder strength was chosen to give a ration of hard to easy direction resistivities equal to 10 at $\nu^* = 0.5$ and the temperature was chosen to be 100 times smaller than the microscopic interaction strength as explained in the text. Interaction and localization effects neglected in this Boltzmann theory are expected to strongly suppress these resistivities at low temperatures outside of the interval $0.4 \lesssim \nu^* \lesssim 0.6$.

The transport theory described above can be readily generalized to account for the non-linear transport features, which are present experimentally - notably at $\nu^* = 1/2$. The voltage drop across a stripe, given by $V_y = aE_y/2$ at $\nu^* = 1/2$, can be readily incorporated into the RG scaling approach for the scattering rates. Not surprisingly, the resulting dependence on voltage is the same as that on temperature obtained above:

$$\begin{aligned} \Gamma_e &\sim \Gamma_e^{(0)}(V_y/E_c)^{2\Delta_e-2} \\ \Gamma_h &\sim \Gamma_h^{(0)}(V_y/E_c)^{2\Delta_h-2}. \end{aligned} \quad (38)$$

This expression is valid in low temperature or high voltage limits, with $k_B T \ll V_y$. The non-linear differential resistivity in the hard direction can now be obtained by using the expression for the tunneling current across stripes from Eq. (34): $I_y = (e^2/h)\Gamma_e V_y L_x/v_F$. One thereby obtains,

$$\frac{\partial V_y}{\partial I_y} \sim I_y^\alpha, \quad (39)$$

with an exponent $\alpha = 2(1 - \Delta_e)/(2\Delta_e - 1)$. Using the value of $\Delta_e = 0.756$ calculated from theory at $\nu^* = 1/2$ for the case $[\nu] = 4$ and $d = 10\ell$ (see Fig. [4], gives the estimate $\alpha = 0.93$. Calculations for models with more remote screening planes will give larger values for Δ_e (but always smaller than one as explained above) and smaller

positive values for α . Notice that a positive exponent implies an enhancement of the hard axis resistivity when driven non-linear - consistent with the experimental findings in Ref. 1. This increase in resistivity is due to a voltage suppression of the correlation induced interlayer tunneling enhancement - and as such is a rather direct experimental indication of non-trivial Luttinger liquid correlations of the chiral edge channels.

A similar calculation can be performed for non-linearities in the easy axis current. At $\nu^* = 1/2$ $V_x \propto \Gamma_e I_x$ where I_x is the easy-direction current. In this case $V_y \propto \nu I_x$ is the Hall voltage. It follows that

$$\frac{\partial V_x}{\partial I_x} \sim I_x^\beta \quad (40)$$

with an exponent $\beta = 2(\Delta_e - 1)$ For $N = 2$ and $d = 10\ell$, we obtain $\beta = -0.48$; smaller negative values are found for models with more remote screening planes. In this theory the easy-direction resistivity is suppressed when driven non-linear with current, a property which is also consistent¹ with experimental findings. We emphasize that these powerlaws hold only in the low-temperature or high-voltage limits; a careful comparison of the theoretical dependence on voltage to temperature ratio with experiment could provide a strong test of this transport theory.

V. SUMMARY

Recent experiments¹⁻³ have established a consistent set of transport properties for high-mobility two-dimensional electron systems with high orbital index ($N \geq 2$) partially filled Landau levels which differ from those in the low orbital index ($N \leq 1$) fractional quantum Hall regime. At large N , the dissipative resistivities are large, strongly anisotropic, and non-linear for $0.4 \lesssim \nu - [\nu] \lesssim 0.6$ within each Landau level. This anisotropic transport regime is bracketed by regions of reentrant integer quantum Hall plateaus. In this paper we have presented a theory which is able to account for most features of these experiments. The theory starts from the unidirectional charge-density-wave (smectic) state of Hartree-Fock theory^{4,5} in which the electrons reside in periodically spaced stripes with a spontaneously chosen orientation. Forward and backscattering interactions, neglected in the Hartree-Fock theory, are included by retaining the low energy electron excitations at the stripe edges. These form a set of coupled 1D chiral modes, easily described with bosonization techniques. We find that: i) for smectic states in quantum Hall systems, the chiral boson degrees of freedom coincide with stripe position and width degrees of freedom; ii) backscattering interactions which drive the system toward electron or hole Wigner crystal states are always relevant, but only below inaccessible low temperatures

in the anisotropic transport regime; and iii) a semiclassical Boltzmann transport theory for the smectic state is able to account for the magnitude of the anisotropic dissipative resistivities and for the sign of the non-linearities which appear at higher transport currents.

VI. ACKNOWLEDGEMENTS

We would like to acknowledge insightful conversations with Herb Fertig, Michel Fogler, Tomas Jungwirth, Jim Eisenstein, Eduardo Fradkin, and Steve Girvin and the stimulating environment provided by the ITP, where this research was initiated. M.P.A.F. is grateful to the NSF for generous support under grants DMR-97-04005, DMR95-28578 and PHY94-07194. A.H.M. is grateful for support under NSF grant DMR-97-14055.

-
- ¹ M.P. Lilly, K.B. Cooper, J.P. Eisenstein, L.N. Pfeiffer, and K.W. West, Phys. Rev. Lett. **82**, 394 (1998); *ibid.* preprint [cond-mat/9903153] (1999); *ibid.* preprint [cond-mat/9903196] (1999).
- ² R.R. Du, D.C. Tsui, H.L. Stormer, L.N. Pfeiffer, K.W. Baldwin, and K.W. West, Solid State Commun. **109**, 389 (1999); W. Pan, R.R. Du, H.L. Stormer, D.C. Tsui, L.N. Pfeiffer, K.W. Baldwin, and K.W. West, preprint [cond-mat/9903160] (1999).
- ³ M. Shayegan and H.C. Manoharan, preprint [cond-mat/9903405] (1999).
- ⁴ A.A. Koulakov, M.M. Fogler, and B.I. Schklovskii, Phys. Rev. Lett. **76**, 499 (1996); Phys. Rev. B **54**, 1853 (1996); M.M. Fogler and A.A. Koulakov, Phys. Rev. B **55**, 9326 (1997).
- ⁵ R. Moessner, and J.T. Chalker, Phys. Rev. B **54**, 5006 (1996).
- ⁶ E.H. Rezayi, F.D.M. Haldane, and Kun Yang, preprint [cond-mat/9903258] (1999).
- ⁷ H.A. Fertig, Phys. Rev. Lett. **82**, 3693 (1999).
- ⁸ Tudor Stanescu, Ivar Martin and Philip Phillips, preprint [cond-mat/9905116] (1999).
- ⁹ See for example T. Jungwirth, A.H. MacDonald, and S.M. Girvin, preprint [cond-mat/9905353] (1999).
- ¹⁰ E. Fradkin and S.A. Kivelson, preprint [cond-mat/9810151] (1998).
- ¹¹ S.A. Kivelson, E. Fradkin, and V.J. Emery, Nature **393**, 550 (1998).
- ¹² See for example V.J. Emery in *Highly Conducting One-Dimensional Solids*, edited by J.T. Devreese, R.P. Evrard, and V.E. van Doren, (Plenum, New York, 1979).
- ¹³ J. Sólyom, Adv. Phys. **28**, 201 (1979).
- ¹⁴ At non-zero temperatures an unbinding of disclinations will destroy the translational LRO, but algebraic rotational order can survive.
- ¹⁵ At $\nu^* = 1/2$ there is an additional class of momentum-

conserving low-energy processes in which one particle scatters across an electron stripe and the second particle across a hole stripe. Calculations similar to those discussed here show that these are irrelevant in a renormalization group sense.

¹⁶ Steven H. Simon, preprint [cond-mat/9903086] (1999).

¹⁷ A.H. MacDonald, unpublished.